MAPLE DEPOSITION OF PLGA MICROSPHERES FOR MEDICAL APPLICATIONS

O. FUFĂ[a,b], M. SOCOL[c], N. PREDA[c], S. GRIGORESCU[a], S. CROITORU[d], G. SOCOL[a*]

[a]*Lasers Department, National Institute for Lasers, Plasma and Radiation Physics, Magurele, Ilfov, Romania*

[b]*Department of Science and Engineering of Oxide Materials and Nanomaterials, Faculty of Applied Chemistry and Materials Science, Politehnica University of Bucharest, Bucharest, Romania*

[c]*Laboratory of Optical Processes in Nanostructured Materials, National Institute of Materials Physics, Magurele, Ilfov, Romania*

[d]*Machines and Manufacturing Systems Department, Faculty of Engineering and Management of Technological Systems, Politehnica University of Bucharest, Bucharest, Romania*

The aim of our study was to synthesize and evaluate the physicochemical and biological properties of composite films based on poly(lactic-co-glycolic acid) copolymer and quercetin (PLGA/Q) microspheres. During our experiments, we firstly synthesized the PLGA/Q microspheres by using an oil-in-water emulsion-diffusion-evaporation method. Subsequently, the as-prepared composite material was subjected to the matrix assisted pulsed laser evaporation (MAPLE) technique, in order to obtain the PLGA/Q coatings. Relevant compositional and microstructural features of the synthesized samples were obtained by means of Fourier transform infrared spectroscopy (FTIR) and AFM (atomic force microscopy). The long-term biocompatibility of the synthesized films was *in vitro* evaluated by cellular viability and immunofluorescence assays.

(Received November 29, 2016; Accepted January 23, 2017)

Keywords: MAPLE, PLGA, quercetin, microspheres, coatings, biocompatible.

1. Introduction

Given the complex etiopathology related to modern healthcare conditions, including herein the intricate genetic cargo of humans and the impressive adaptation capacity of pathogens, the current conventional drug therapy can be often associated with alarming drawbacks and potential side effects [1,2]. Therefore, in the cumulative context of the ineffective therapeutic strategies and the tremendous versatility and outcome of nanotechnologies, the scientific community and healthcare professionals gathered their knowledge and efforts towards the development and promotion of novel drug-based systems, contributing thus to the implementation and progress of modern personalized medicine [3-5]. Such nanotechnology-related structures require versatile biomaterials with tunable features, complex architectonics and genuine load/release mechanism which may provide targeted and controlled delivery of therapeutic agents [6,7].

The nanotechnology-derived polymer structures experimentally proved to represent ideal candidates for novel biomedical-related applications thanks to their specific compositional and structural features, intrinsic biocompatibility and versatile properties (including herein easy processability, attractive physicochemical features and tunable functionalization processes, all governed by their specific high surface/volume ratio) [8,9]. In particular, the interest straightened towards biodegradable natural and synthetic polymers have gained significant importance, since such biomaterials can be *in vivo* degraded either by enzymatic or non-enzymatic mechanisms

* Corresponding author: gabriel.socol@inflpr.ro

[10,11] and proved promising potential for innovative and effective bioactive substance delivery systems [12,13], antimicrobial and antitumor therapies [14,15] and tissue engineering applications [16,17].

Quercetin is a plant-derived flavonoid with an enhanced anti-oxidative activity that is widely used as an ingredient in food industry and pharmacology, particularly for tissue regeneration [18,19] and for prevention and treatment of cancer [20,21,22] and degenerative diseases [23,24]. Given the intrinsic antimicrobial effects of quercetin, related to its specific binding to bacterial DNA gyrase, this flavonol compound is also used as a promising tool against bacterial contamination [25,26,27]. In combination with some drugs for a certain amount, quercetin may present harmful side effects. The control of its release is an important parameter for the used in drug delivery applications. The embedding the quercetin into the polymeric matrix in form of the microspheres could reduce its cytotoxicity. In our study we showed that the polymeric microspheres can be laser transferred as coatings conserving the morphology of the particulates and their chemical composition.

2. Materials and Methods

2.1. Materials

Poly(lactic-co-glycolic acid) copolymer (PLGA) with 50:50 lactic to glycolic acid molar ratio was purchased from Sigma Aldrich. Analytical graded ethyl acetate ($C_4H_8O_2$), acetone (C_6H_6O), ethanol (C_2H_6O) and hexane (C_6H_{14}) were also provided by Sigma Aldrich. The required glass and high purity (100) silicon substrates were purchased from a local supplier.

Dulbecco's Modified Eagle Medium (DMEM), phosphate buffered saline (PBS), fetal bovine serum (FBS) and penicillin/streptomycin (P/S) antibiotic mixture were purchased from Biochrom. The AB viability assay kit (alamarBlue® Cell Viability Assay Protocol) was acquired from Thermo Scientific, while the phalloidin-FITC (fluorescein isothiocyanate green-labeled phalloidin) and DAPI (2-(4-amidinophenyl)-6-indolecarbamidine dihydrochloride) stains were purchased from Sigma-Aldrich.

2.2. Methods

2.2.1. Synthesis of PLGA/Q microspheres

For the experimental microencapsulation of quercetin within the polymer structures (PLGA/Q) we selected an oil-in-water (o/w) emulsion-diffusion method, followed by solvent evaporation. In this respect, we firstly obtained the PLGA and quercetin solutions by dissolving the polymer in ethyl acetate (20 mg/mL) and by dispersing the flavonol compound in deionized water (10 mg/mL). Subsequently, the PLGA-based solution was added into the quercetin-containing aqueous solution and the resulted mixture was subjected to vigorous sonication (3 minutes at 50% amplitude) and stirring (3 hours at room temperature conditions) processes. Finally, the as-prepared systems were centrifuged for 15 minutes and subjected to a triple washing treatment with deionized water. The same synthesis recipe was applied to synthesize pristine PLGA-based microspheres.

2.2.2. Synthesis of PLGA/Q microspheres-based coatings

The previously synthesized PLGA/Q systems were suspended in hexane, in order to obtain a colloidal suspension of 30 mg/mL concentration which was further frozen at liquid nitrogen temperature for 30 minutes. The resulted frozen materials were placed onto the constituent cooling system inside the reaction chamber of the MAPLE experimental setup, which enabled the maintenance at liquid nitrogen temperature of the targets during the deposition. All the experiments were performed by using a KrF* excimer laser source (λ = 248 nm, τ_{FWHM} = 25 ns) from Lambda Physics, Coherent. The depositions were conducted at room temperature conditions at 0.1 Pa background pressure inside the reaction chamber, by keeping constant the target-substrate distance (5 cm), the frequency of laser beam (20 Hz) and the applied number of pulses (50,000).

In order to emphasize the physicochemical properties of the laser transferred composite materials, we also performed MAPLE experiments on pristine PLGA microspheres by using the same deposition parameters, but also comparative dropcast experiments from the same

concentration of PLGA/Q microspheres suspended in hexane onto IR transparent silicon substrates.

2.3. Physicochemical characterization

2.3.1. Fourier Transform Infrared Spectroscopy (FTIR)

In order to investigate the chemical composition and structural integrity of the obtained PLGA/Q samples, we performed comparative FTIR studies on laser-processed and dropcast specimens. The required measurements were performed by recording 50 individual scans per sample between (4000 – 500) cm^{-1} wavenumbers with a 4 cm^{-1} resolution. The data were collected in the transmission mode by using a Shimadzu 8400S Spectrometer.

2.3.2. Atomic Force Microscopy (AFM)

The specific surface-related features of the synthesized PLGA/Q films were experimentally investigated by means of AFM technique. In this respect, a 4000 Multiview System purchased from Nanonics Imaging Ltd. Company was used to record data from an interest area of 5 μm x 5 μm for each sample, in the tapping mode.

2.4. Biological evaluation

In order to assess the biocompatibility of the PLGA/Q films synthesized by MAPLE, we experimentally performed *in vitro* quantitative and qualitative assays on preosteoblast mouse-derived MC3T3 mesenchymal cell line. Prior to the required experiments, the cells were cultivated in DMEM supplemented with P/S mixture and FBS under standard conditions (37 ± 2^{o}C, 5 ± 1% CO_2, more than 90% humidity), until confluence. Afterwards, the cells were washed 3 times with PBS, detached, placed in fresh culture medium and counted. Before the experiments, the samples and controls (uncoated glass slides) were sterilized by UV light treatment.

2.4.1. Cellular viability assay

Relevant quantitative data regarding the proliferation of the experimentally treated MC3T3 cells were acquired by performing Alamar Blue (AB) cellular viability assay. This assay involves the optical correlation between the viable cells and the amount of resorufin (a red fluorescent product resulted after the mitochondria-mediated reduction of blue resazurin by NADPH or NADH cofactors from active cells).

In this respect, all the samples (uncoated glass slides and glass substrates coated with pristine PLGA films and microsphere-based PLGA/Q films) were placed in 12 well plates. Subsequently, 5,000 cells in culture medium were seeded in each well and cultured for under standard conditions (37^{o}C, 5% CO_2, humid atmosphere) for various time periods: 1, 3, 4, 5, 6, 7, 8, and 11 days. After the incubation period, the culture medium was removed and replaced with the same volume of fresh medium (consisting in MEM, FBS, P/S mixture and AB solution). The cells were thus incubated for 3 hours in dark conditions and the resulted solutions were further transferred in 96 well plates. In order to estimate the viable cells, the absorbance of the resulted solutions was read at 570 and 600 nm by using a Mithras LB940 microplate reader from Thermo Scientific. The results are presented as the average absorbance of three individual measurements.

2.4.2. Immunofluorescence assay

In order to assess the qualitative biocompatibility of the samples, fluorescence microscopic evaluation of the treated MC3T3 cells was performed. The selected immunofluorescence staining protocol enabled us to investigate the morphology of the cells, thanks to the beneficial conjunction of phalloidin-FITC (green-labeled dye with specific action for coupling and stabilization of F-actin filaments within the cellular cytoskeleton) and DAPI (blue fluorescent compound with enhanced affinity for the genetic cargo).

All the samples in our experiments were placed in 12 well plates, inoculated with 5,000 cellular densities and cultivated in standard conditions for distinctive time periods, namely 1 up to 8 days. The treated specimens were subjected to a standard washing and fixing treatment, followed by the addition of the fluorescent stains and 2-hour incubation under dark conditions. After an additional washing treatment with PBS, the samples were investigated by fluorescence microscopy means, using in this respect an IX71 instrument from Olympus.

3. Results and discussions

The FTIR spectra of the experimentally synthesized PLGA/Q films (obtained by both MAPLE and dropcast methods) are presented in Fig. 1. In both spectra, the broad band between 3100 and 3600 cm^{-1} is specifically assigned to the overlapped stretch of free O–H group within both organic compounds. When compared to the dropcast PLGA/Q sample, the after-mentioned infrared band is more intense in the case of MAPLE-derived film; this remark suggests the abundance of hydroxyl group within the laser-assisted synthesized samples, which may represent a promising site for subsequent physical-guided functional interactions. Also, the sharp infrared maxima observed within the functional group region at ~3000 and ~2950 cm^{-1} wavenumbers correspond to the asymmetric stretching vibrations of $–CH_3$ and $–CH_2–$ within the copolymer, respectively [28]. The intense vibrational peak at ~1760 cm^{-1} wavenumber is specifically attributed to the overlapping stretching vibrations of carbonyl functional groups within the aldehyde and ketone functional groups of PLGA and quercetin, respectively [29,30]. Specific infrared bands of the flavonol compound are present at ~1660 cm^{-1} (typical stretching vibrations of C=O aryl ketones), ~1610 and ~1510 cm^{-1} (specific stretch of C=C bonds within the constituent aromatic rings) [31,32]. The infrared peak at ~1370 cm^{-1} may be assigned to the overlapping of weak –OH and $–CH_3$ bending vibrations of the phenol and methyl functions in quercetin and PLGA, respectively [33]. The weak vibrational bands identified between ~1320 and ~1130 cm^{-1} wavenumbers may be attributed to the symmetric and asymmetric stretching vibrations of C–O and C–O–C functional groups within the copolymer, while the very weak vibrational maxima identified between ~930 and ~990 cm^{-1} wavenumbers may be assigned to the bending vibrations of terminal alkenes within PLGA composition [34]. Out of plane bending vibrations of hydroxyl and methyldyne functional groups are present at wavenumber values between 880 and 600 cm^{-1}.

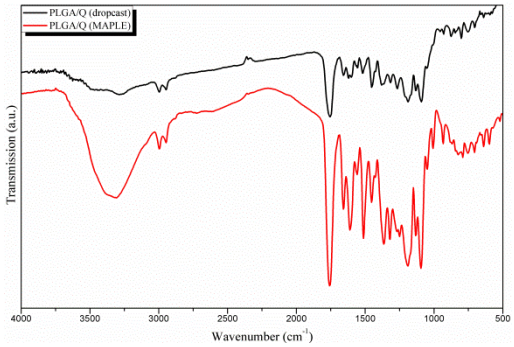

Fig. 1: FTIR spectra of the PLGA/Q coatings.

When compared to the infrared data of pristine PLGA and quercitin, no additional transmission maxima are identified in the current spectra, suggesting thus the sole physical interactions established between the two compounds. As one can notice, all the vibrational maxima identified in the PLGA/Q spectra are more intense in the case of MAPLE-derived samples; this observation may be related to the increased amount of quercetin within the synthesized films (which is also dependent on the thickness of the samples), suggesting thus the successful laser-assisted transfer of composite materials based on copolymer and flavonol onto the substrates.

Relevant data regarding the topography of the PLGA/Q films obtained by MAPLE are pictured in the AFM micrographs from Fig. 2. The surface of the PLGA sample seems rather discontinuous, being comprised by segregate vault-shaped polymer structures and spacious copolymer-free regions. When compared to the pristine PLGA sample, the microsphere-based film obtained by laser processing uniformly covers the entire surface of the substrate, while the surface seems rather irregular, being organized in dome-like structures of various nanosized dimensions. With respect to the PLGA/Q sample, one can observe the abundance of spherical-shaped copolymer/flavonol structures, but also the presence of few larger aggregate structures which may

be the result of the irregular rearrangement of microspheres after the interactions between the frozen target and the laser beam. Both samples have rough surfaces, with a slightly more abrasive topography in the case of PLGA/Q film, the maximum roughness being estimated around 500 nm. The experimentally evaluated roughness of PLGA/Q sample represent an essential feature related to the hydrophilic/hydrophobic behaviour of the MAPLE-derived film and to future auspicious interactions with cells.

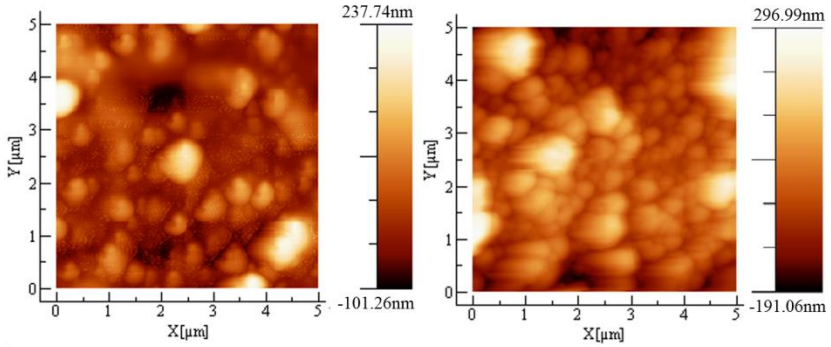

Fig. 2: AFM images of the PLGA and PLGA/Q coatings.

The cellular viability assay results corresponding to the preosteoblast cells treated in the presence of our experimental samples are presented in Fig. 3. When considering the uncoated glass samples, one can observe that the cellular population exponentially increased during the first 8 days of the experiment and reached a viability plateau until the end of the experiment. One may assume that, after 8 days of *in vitro* treatment, the MC3T3 cells entirely covered the surface of the glass slides and the cells reach confluence. A similar behaviour can be observed for the pristine PLGA films deposited onto glass substrates, where the typical plateau related to the highest number of viable cells onto the samples is also reached after 8 days of experiment. In this particular case, the absorbance (directly related to the number of living cells) corresponding to the 1st and 8th days of treatment is comparable to the control data, suggesting thus the biocompatible feature of the PLGA-based samples. Since the absorbance values measured for the pristine PLGA films during days 2 and 7 of the treatment are lower than the values corresponding to the control at same time periods, one may assume that the proliferation rates of the cells are slightly distinctive and may be due to the initial chemical reorganization of PLGA onto the surface of the glass substrate. Interesting fact that after the 8th day of experimental treatment, the number of viable cells corresponding to the PLGA samples is higher than the glass control, which may be assigned to a local dissolution of the polymer film within the cellular medium and the subsequent attachment and proliferation of MC3T3 cells onto the as-exposed surface. In contrast with the bare and PLGA-coated glass samples, only a slight increase in the number of viable cells is reported in the case of PLGA/Q samples during the first 3 days of experiment. Starting from the 3rd day of experiment until the 8th day, the viability of the cells treated in the presence of the polymer/flavonol specimens is slightly altered, the measured absorbance values being below the cytotoxicity restriction. Since the number of viable cells slowly increased during the last days of the experiment, one may assume either that the inoculated cells did not access the entire surface of the sample from the beginning of the experiment or that significant chemical and morphological rearrangement of the PLGA/Q film occurred after the initial experimental period (enabling thus the cells to attach and proliferate onto newly exposed areas from the glass substrates). Or, one may assume that – after 3 days of incubation – the PLGA/Q samples exhibit a slightly cytotoxic behaviour on MC3T3 cells. By making this assumption, one can also presume the validity of the „rearrangement period" occurred during days 4 to 8, which might have allowed the viable cells to specifically interact with the composite microspheres. By doing so, the cellular uptake of quercetin seems a valid assumption, as well as its further beneficial antioxidant activity within the cells, which might have further encouraged the revival of the cellular proliferation process.

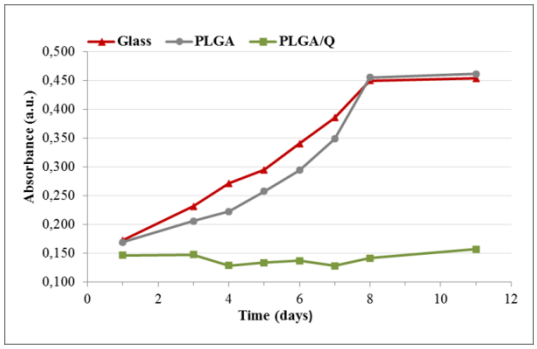

Fig. 3: Cellular viability results of the PLGA and PLGA/Q coatings.

Representative immunofluorescence micrographs depicting the morphology of the MC3T3 cells treated in the presence of uncoated and coated glass slides can be observed in Fig. 4. The fluorescence images corresponding to uncoated and PLGA-coated glass substrates are quite similar during the same periods of the experimental treatment and suggest the abundance and uniform distribution of MC3T3 cells onto the entire surface of the samples. The micrographs obtained after 8 days of inoculations rather indicate the cellular overpopulation onto the samples, this observation being in compliance with the previously discussed cellular viability results. After the first day of treatment, one can notice that the identified cells still possess particular fibroblast-like features: preferentially longitudinal-disposed and locally branched actin filaments cytoplasm (corresponding to cellular body and projections, respectively), central elliptical prominent nuclei, overspread and flattened morphology, typical parallel cluster alignment. However, the micrographs performed after 3 days of experiments fully reveals specific osteoblast-like phenotype: the green-labeled actin filaments possess preferential branched disposal and delimit the flattened and extensive cytoskeleton of osteoblast, while the identified round to oval shaped nuclei are preferentially located in the periphery of the cells.

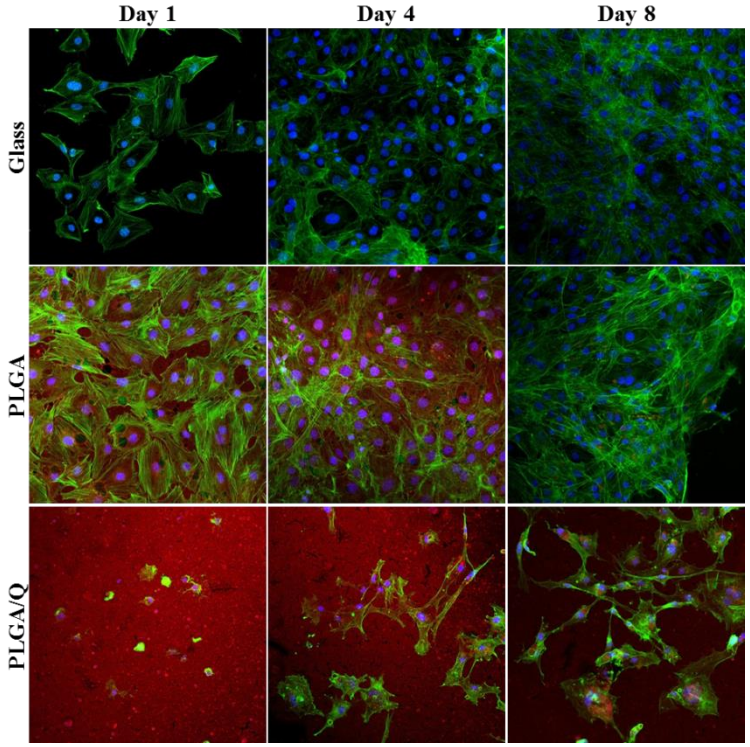

Fig. 4: Fluorescence micrographs of the PLGA and PLGA/Q coatings.

The deficiency of MC3T3 cells onto the surface of the PLGA/Q samples observed in the fluorescence micrographs is in compliance with the cellular viability results. After the first day of *in vitro* experiments, few isolated constricted cells are identified onto the surface of the samples. After the 3rd day of treatment, one can notice the specific osteoblast-like flattened morphology of the cells and a slightly increase of the cellular population. The beneficial cellular proliferation of the treated cells can be clearly observed after 8 days of treatment. In this particular case, one can distinguish the osteoblast-like phenotype of the cells, but also the presence of dark orange aggregate structures inside the cells. If considering the fluorescence phenomena related to the selected flavonol, the identified microsized aggregates may be due to the cellular internalization of quercetin. Therefore, our previous assumption regarding a 3-stage biocompatible behavior of the MAPLE-synthesized PLGA/Q films becomes valid.

4. Conclusions

The MAPLE technique has proved to be an efficient method for the deposition of PLGA and quercetin-embedded PLGA microspheres. The AFM investigations demonstrated that the morphological features (shape and size) of the polymeric particles were preserved after their laser transfer as coatings onto various substrates. Moreover, the FTIR spectra confirmed that the chemical composition of the constituent compounds after MAPLE deposition was the same with the pristine powders. Biocompatibility assay showed that the coatings based on PLGA microsphere are not cytotoxic for MC3T3 cells, revealing a similar behaviour with the control samples (bare glass). The MC3T3 cells entirely covered the surface of the PLGA coatings reaching the confluence after 8 days from inoculation.

The fluorescence images showed a good spreading and a normal cell morphology that indicates a good cell adhesion on our PLGA microspheres based coatings. These results encourage further assessment of such structures for application in drug release at implantation sites. The quercetin embedding into the PLGA matrix of microspheres has limited the growth of the MC3T3 cells in the first days of cell incubation, most likely due to the large amount of the flavonoid released into the cell culture medium.

Acknowledgments

The work has been funded by the Romanian National Authority for Scientific Research, CNCS-UEFISCDI, projects no. TE 188/2014 - PN-II-RU-TE-2014-4-1590, 153/ 07.09.2012 - PN-II-PT-PCCA-2011-3.2-0898 and the National Authority for Research and Innovation in the frame of Nucleus Programme - contract 4N/2016.

References

[1] P. Khadka, J. Ro, H. Kim, I. Kim, J.T. Kim, H. Kim, J.M. Cho, G. Yun, J. Lee, Asian J Pharm Sci **9**, 304 (2014).
[2] J. Safari, Z. Zarnegar, J Saudi Chem Soc **18**, 85 (2014).
[3] C.L. Hastings, E.T. Roche, E. Ruiz-Hernandez, K. Schenke-Layland, C.J. Walsh, G.P. Duffy, Adv Drug Deliv Rev **84**, 85 (2015).
[4] J. Bruix, K.H. Han, G. Gores, J.M. Llovet, V. Mazzaferro, J Hepatol **62**, 144 (2015).
[5] P. Zhou, X. Sun, Z. Zhang, "Kidney–targeted drug delivery systems", Acta Pharm Sin B **4**(1), 37 (2014).
[6] S.S. Ajazuddin, Fitoterapia **81**, 680 (2010).
[7] S.R. Mudshinge, A.B. Deore, S. Patil, C.M. Bhalgat, Saudi Pharm Journal **19**, 129 (2011).
[8] K.S. Kim, B. Duncan, B. Creran, V.M. Rotello, NanoToday **8**, 439 (2013).
[9] S. Sharma, A. Singh, "Nanotechnology Based Targeted Drug Delivery: Current Status and

Future Prospects for Drug Development, Drug Discovery and Development - Present and Future", edited by I.M. Kapetanović, ed. InTech, Rijeka, Croatia, 427-462 (2011).
[10] F. Puoci, G. Cirillo, M. Curcio, O.I. Parisi, F. Iemma, N. Picci, Expert Opin Drug Deliv **8**(10), 1379 (2011).
[11] O.S. Kluin, H.C. van der Mei, H.J. Busscher, D. Neut, Expert Opin Drug Deliv **10**(3), 341(2013).
[12] X.B. Dou, Y. Hu, N.N. Zhao, F.J. Xu, Biomaterials **35**(9), 3015 (2014).
[13] G.A. Foster, D.M. Headen, C. González-García, M. Salmerón-Sánchez, H. Shirwan, A.J. García, Biomaterials **113**, 170 (2016).
[14] V. Grumezescu, A.M. Holban, F. Iordache, G. Socol, G.D. Mogoşanu, A.M. Grumezescu, A. Ficai, B.Ş. Vasile, R. Truşcă, M.C. Chifiriuc, H. Maniu, , Appl Surf Sci **306**, 16 (2014).
[15] D. Rădulescu, V. Grumezescu, E. Andronescu, A.M. Holban, A.M. Grumezescu, G. Socol, A.E. Oprea, M. Rădulescu, A. Surdu, R. Truşcă, R. Rădulescu, M.C. Chifiriuc, M.S. Stan, S. Constanda, A. Dinischiotu, Appl Surf Sci **374**, 387 (2016).
[16] M.E. Hoque, T.T.H. Meng, Y.L. Chuan, M. Chowdhury, R.G.S.V. Prasad, Mater Lett **131**, 255 (2016).
[17] P. Bhattacharjee, D. Naskar, T.K. Maiti, D. Bhattacharya, S.C. Kundu, Appl Mater Today **5**, 52 (2016).
[18] L. Mohan, C. Anandan, N. Rajendran, Int J Biol Macromolec **93**(B), 1633 (2016).
[19] S.K. Gupta, R. Kumar, N.C. Mishra, Mater Sci Eng C **71**, 919 (2017).
[20] C. Caddeo, A. Nacher, A. Vassallo, M.F. Armentano, R. Pons, X. Fernàndez-Busquets, C. Carbone, D. Valenti, A.M. Fadda, M. Manconi, Int J Pharm **513**(1-2), 153 (2016).
[21] M. Lou, L. Zhang, P. Ji, F. Feng, J. Liu, C. Yang, B. Li, L. Wang, Biomed Pharmacother **84**, 1 (2016).
[22] J.Y. Kee, Y.H. Han, D.S. Kim, J.G. Mun, J. Park, M.Y. Jeong, J.Y. Um, S.H. Hong, Phytomedicine **23**(13), 1680 (2016).
[23] D. Sun, N. Li, W. Zhang, Z. Zhao, Z. Mou, D. Huang, J. Liu, W. Wang, Colloids Surf B **148**, 116 (2016).
[24] L. Cui, Z. Li, X. Chang, G. Cong, L. Hao, Vascul Pharmacol **88**, 21 (2016).
[25] A. Plaper, M. Golob, I. Hafner, M. Oblak, T. Tomaž Šolmajer, R. Jerala,Biochem Biophys Res Commun **306**(2), 530 (2003).
[26] P.S. Bustos, R. Deza-Ponzio, P.L. Páez, I. Albesa, J.L. Cabrera, M.B. Virgolini, M.G. Ortega, Environ Toxicol Pharm 48, **253** (2016).
[27] X. Yang, W. Zhang, Z. Zhao, N. Li, Z. Mou, D. Sun, Y. Cai, W.Wang, Y. Lin, J Inorg Biochem **167**, 36 (2917).
[28] M.L. Amin, D. Kim, S. Kim, Eur J Pharm Sci **91**, 138 (2016).
[29] N. Ignjatović, V. Wu, Z. Ajduković, T. Mihajilov-Krstev, V. Uskoković, D. Uskoković, Mater Sci Eng C **60**, 357 (2016).
[30] M. Catauro, F. Bollino, P. Nocera, S. Piccolella, S. Pacifico, Mater Sci Eng C **68,** 205 (2016).
[31] V.S.S. Gonçalves, S. Rodríguez-Rojo, E. De Paz, C. Mato, A. Martín, M.J. Cocero, Food Hydrocolloids **51**, 295 (2015).
[32] G. Wang, J.J. Wang, X.L. Chen, L. Du, F. Li, J Control Release **235**, 276 (2016).
[33] C. D'Avila Carvalho Erbetta, R.J. Alves, J. Magalhães Resende, R.F. de Souza Freitas, R.G. de Sousa, J Biomater Nanobiotechnol **3**(2), 208 (2012).
[34] N. Rescignano, L. Tarpani, A. Romani, I. Bicchi, S. Mattioli, C. Emiliani, L. Torre, J.M. Kenny, S. Martino, L. Latterini, I. Armentano, Polym Degrad Stab **134**, 296 (2016).